**Title:** Olfactory Neuroepithelium Cells from Cannabis Users Display Alterations to the Cytoskeleton and to Markers of Adhesion, Proliferation and Apoptosis

**Running Title:** Olfactory Neuroepithelium Cells from Cannabis Users

Alejandra Delgado-Sequera[1,2#], María Hidalgo-Figueroa[1,2,3#], Marta Barrera-Conde[4,5], Mª Carmen Duran-Ruiz[2,6], Carmen Castro[2,6], Cristina Fernández-Avilés[5], Rafael de la Torre[4,6,7], Ismael Sánchez-Gomar[2,6], Víctor Pérez[3,8], Noelia Geribaldi-Doldán[2,9], Patricia Robledo*[4,5] and Esther Berrocoso*[1,2,3]

[1]Neuropsychopharmacology and Psychobiology Research Group, Department of Psychology, University of Cádiz, Cádiz, Spain.
[2]Instituto de Investigación e Innovación Biomédica de Cádiz, INiBICA, Hospital Universitario Puerta del Mar, Cádiz, Spain.
[3]Centro de Investigación Biomédica en Red de Salud Mental (CIBERSAM), Instituto de Salud Carlos III, Madrid, Spain.
[4]Integrative Pharmacology and Systems Neuroscience, IMIM-Hospital del Mar Research Institute, Barcelona, Spain.
[5]Department of Experimental and Health Sciences, University Pompeu Fabra, Barcelona, Spain.
[6]Biomedicine, Biotechnology and Public Health Department, University of Cádiz, Cádiz, Spain.
[7]Centro de Investigación Biomédica en Red de Fisiopatología de la Obesidad y Nutrición, Instituto de Salud Carlos III, Madrid, Spain.
[8]Neuropsychiatry and Addictions Institute (INAD) of Parc de Salut Mar, Barcelona, Spain.
[9]Departament of Human Anatomy and Embriology, University of Cádiz, Cádiz, Spain.

# These authors have contributed equally to this work

***Corresponding authors:** Esther Berrocoso, Department of Psychology, Campus Universitario Río San Pedro s/n, 11510-Puerto Real (Cadiz), Spain. Tel.: +34956015224; Fax: +34956015225; e-mail: esther.berrocoso@uca.es; Patricia Robledo, Neurosciences Research Programme, IMIM-Hospital del Mar Research Institute. PRBB, Calle Dr. Aiguader 88, Barcelona 08003, SPAIN. probledo@imim.es Tel: +34 93 316 0455

**ABSTRACT**

Cannabis is the third most commonly used psychoactive substance of abuse, yet it also receives considerable attention as a potential therapeutic drug. Therefore, it is essential to fully understand the actions of cannabis in the human brain. The olfactory neuroepithelium (ON) is a peripheral nervous tissue that represents an interesting surrogate model to study the effects of drugs in the brain, since it is closely related to the central nervous system, and sensory olfactory neurons are continually regenerated from populations of stem/progenitor cells that undergo neurogenesis throughout life. In this study, we used ON cells from chronic cannabis users and healthy control subjects to assess alterations in relevant cellular processes, and to identify changes in functional proteomic pathways due to cannabis consumption. The ON cells from cannabis users exhibited alterations in the expression of proteins that were related to the cytoskeleton, cell proliferation and cell death, as well as, changes in proteins implicated in cancer, gastrointestinal and neurodevelopmental pathologies. Subsequent studies showed cannabis provoked an increase in cell size and morphological alterations evident through β-Tubulin III staining, as well as, enhanced beta-actin expression and a decrease in the ability of ON cells to undergo cell attachment, suggesting abnormalities of the cytoskeleton and cell adhesion system. Furthermore, these cells proliferated more and underwent less cell death. Our results indicate that cannabis may alter key processes of the developing brain, some of which are similar to those reported in mental disorders like DiGeorge syndrome, schizophrenia and bipolar disorder.

**Keywords:** Cannabis, human olfactory neuroepithelium, proteomic, cytoskeleton, adhesion, apoptosis

**DECLARATIONS:**

**Funding:** This study was supported by grants co-financed by the "Fondo Europeo de Desarrollo Regional" (FEDER)-UE "A way to build Europe" from the "Programa Operativo de Andalucía FEDER, Iniciativa Territorial Integrada ITI 2014-2020 Consejería Salud, Junta de Andalucía" (PI-0009-2017); the "Consejería de Economía, Innovación, Ciencia y Empleo de la Junta de Andalucía" (CTS-510); Plan Nacional sobre Drogas (2019I041), the "Ministerio de Economía, Industria y Competitividad ("Juan de la Cierva Incorporación" postdoctoral grant I JCI-2015-23280), the "Centro de Investigación Biomédica en Red de Salud Mental-CIBERSAM" (CB/07/09/0033; CB/07/09/0029), and Instituto de Salud Carlos III, Ministerio de Ciencia e Innovación de España y fondos FEDER (PI18/00053 to P.R.).

**Availability of data and material:** This Declaration acknowledges that this paper adheres to the principles for transparent reporting and scientific rigour of preclinical research as stated in the BJP guidelines for Design and Analysis, Immunoblotting and Immunochemistry, and as recommended by funding agencies, publishers and other organisations engaged with supporting research.

**Author's contribution:** ADS and MHF performed the experiments, collected and analysed the data and prepared the original draft of the manuscript; MCDR and ISG collaborated on the proteomics studies and the studies of apoptosis; CC and NGD collaborated with the cell cultures and immunocytochemical studies; CFA and MBC initially processed the samples and handled the primary cell cultures. PR and RT participated in planning the experiment, and provided financial support. ACR performed the neuropsychological evaluation; EB designed and supervised the research study and wrote the manuscript. All the authors reviewed and approved the final version of the manuscript submitted.

**Conflicts of interest/Competing interests:** Not applicable

**Ethics approval:** The study was reviewed and approved by the local institutional ethics committee (CEIC-PSMAR). All subjects provided their written informed consent after the study and procedures were explained to them in full.

## 1. INTRODUCTION

Cannabis is the most widely used illicit substance worldwide, and both the use and misuse of this substance is increasing in many countries. In Europe, the lifetime prevalence of cannabis use is about five times higher than that of other illicit. Many concerns have been raised regarding the adverse effects of cannabis use during adolescence, with suggestions that it may lead to the development of substance use disorders or mental disorders, such as psychosis, depression, bipolar disorder or anxiety [1]. However, there is data arguing that cannabis is a safe and natural alternative for the treatment of a variety of medical and mental health conditions [2]. Thus, one of the outstanding challenges is to define the neuropathological mechanisms specifically altered by cannabis that may trigger psychiatric conditions in vulnerable populations. Unfortunately, despite the enormous amount of information coming from animal models, genetic and human neuroimaging data [3, 4], there is still an important lack of information from human neuronal tissue and live cells that addresses the effects of cannabis in the nervous system.

In adulthood, the differentiation of precursor cells into neurons continues in several brain structures and in some peripheral tissue, such as the olfactory neuroepithelium (ON). In the ON, olfactory sensory neurons are continually regenerated throughout life from stem or progenitor cells by neurogenesis, these populations located at the apical and basal membranes [5]. Thus, the ON contains multipotent cells that can proliferate *in vitro* and that can differentiate into multiple cell types, including neurons and glia [6]. As they can be easily collected through nasal brushing, several studies have demonstrated the utility of the ON as a surrogate tissue to investigate disease related events that affect neurons in the brain. For example, cells isolated from the ON have been used to study the molecular profiles associated with such disease states, showing alterations to cell signalling pathways involved in cell proliferation, neurogenesis and cell adhesion in schizophrenia [7, 8]. In bipolar disorder, the cell death of ON cells is enhanced, and these cells display alterations of the cytoskeleton and in cell migration [8-10]. In the field of cannabis, we previously showed that ON cells obtained from cannabis users exhibit changes in the cannabinoid CB1 receptor, and in serotonin 2A receptor heteromer expression and function, both of which were associated with cognitive performance [11]. Furthermore, the macromolecular profile of ON cells is also altered in cannabis users, these cells displaying a modified lipid composition, as well as an increase in DNA and histone methylation [12]. Thus, these data demonstrate that this peripheral tissue can be used as a surrogate model of the central nervous system (CNS) function, and may provide relevant information related to the neuropathology observed in different mental illnesses including substance-related disorders.

The objective of this study was to explore the effects of prolonged cannabis use on protein expression in ON cells, since they may be related with CNS alterations in neuropsychiatric disorders.. Thus, we examined changes in relevant cellular processes, and adopted a label-free proteomic approach to identify potential changes in functional pathways in ON cells as result of prolonged cannabis consumption.

## 2. MATERIALS AND METHODS

### 2.1. Subjects

Six cannabis users and 7 control subjects were recruited at the IMIM-Hospital del Mar Research Institute (Barcelona, Spain). All subjects provided their written informed consent after the study and procedures were explained to them in full. All the subjects, of either sex, were between 18 and 40 years old, and the cannabis users consumed 5 or more cannabis cigarettes per week. Subjects were instructed to abstain from cannabis use for at least 12 h before testing. The subjects were excluded if they fulfilled any of the following criteria: (1) comply with the criteria for any severe mental disorder according to DSM-V; (2) any history of severe congenital, medical or neurological illness; (3) a history of severe mental illness among first degree relatives; (4) consumption of other drugs of abuse except alcohol and tobacco. In order to exclude subjects with an acute intoxication with psychoactive substances, which could modify the results of the neuropsychological tests, urine concentrations of tetrahydrocannabinol (THC), barbiturates, cocaine, amphetamine, benzodiazepines and opioid metabolites, were measured using the Instant-View, Multipanel 10 Test Drug Screen (Alfa Scientific Designs, USA); and (5) present any medical condition with nasal repercussions (rhinitis or bleeding). The exclusion criteria were verified using the Hamilton Depression Rating Scale (HDRS-17), the individual's clinical history and a diagnostic interview according to DSM-V criteria (SCID). Furthermore, a Neurological Evaluation Scale was used to evaluate neurological soft signs (NSS) [13] and the Global Assessment of Functioning scale (GAF) was used to measure the level of functionality [14].

### 2.2. Neuropsychological evaluation

Neuropsychological tests were performed to assess cognitive functioning. To evaluate attention, the spatial span direct recall with the Cambridge Neuropsychological Test Automated Battery (CANTAB) (Cambridge Cognition, 2017) and the digit span direct recall (WAIS-III) [15] tests were used. These analyses were performed with the measures of span length. Spatial span inverse recall (CANTAB) and the digit span inverse recall (WAIS-III) tests were used to assess working memory. The emotion recognition task (ERT, CANTAB) was used to determine social and emotional cognition, the semantic verbal fluency test (SVFT) [16] was used for executive functions, and the vocabulary test (WAIS-III) was used to estimate premorbid intelligence.

### 2.3. Measurement of cannabis consumption in plasma

To estimate cannabis consumption, THC and its metabolites, 11-hydroxy-THC (11-OHTHC) and 11-nor-9-carboxy-Δ-9-THC (THC-COOH) were quantified in plasma, as reported previously [11]. We followed the Waters Corporation protocol with some modifications [17]. Briefly, 1 ml of plasma was spiked with an internal standard d3-Δ-9-THC (10 µl of 1 µg/ml solution in MeOH), and the protein was precipitated with 2 ml of 0.1% formic acid in acetonitrile and centrifuged for 10 minutes at 3,500 rpm. The supernatant was diluted in 4 ml of MilliQ water and loaded to an Oasis Prime HLB 3 $cm^3$, 60 mg column (Waters Co., USA). To wash the column, 2 ml of 25% methanol was added and it was eluted by adding 2 ml of 90:10 acetonitrile:methanol twice. A nitrogen stream was used at <39 °C and <15 psi pressure to dry the organic phase. Analytes were reconstituted in 50 µl of 90:10 ACN:MeOH and 50 µl of MilliQ

water, and THC and its metabolites were quantified in an Agilent 1200 series HPLC system coupled to a 6410 Triple Quadrupole LC-MS (Agilent Technologies, USA) mass spectrometer with an electrospray interface. Nitrogen was employed as a drying and nebulizing gas.

**2.4. Nasal brushing and cell culture**

Cells were exfoliated from the nasal cavity as described previously [11], using specific brushes to obtain samples from the lower and middle turbinate through a circular movement. Cells were grown at 37 °C and with 5% $CO_2$ in Dulbecco's Modified Eagle Medium/Ham F-12 (DMEM/F12) containing 10% Fetal Bovine Serum (FBS), 2% GlutaMAX 100X and 1% antibiotic-antimycotic (Thermo Scientific, Spain). When confluent, the cells were detached with 0.25% trypsin-EDTA (GibcoBRL, USA), and about 200,000 cells were re-plated in 75 $cm^2$ flasks and cultured in supplemented medium. Independent cell cultures were performed for each subject. All experiments were carried out on cells cultured to passage 6.

**2.5. Sample preparation for proteomic analysis**

ON cells were cultured under proliferative conditions for five days and then lysed (1 $x10^6$ cells per condition) in lysis buffer for protein extraction: 1% NP40, 50 mM HEPES [pH 7], 150 mM NaCl, 1 mM EDTA, supplemented with protease inhibitors. Proteins (100 µg/sample) were precipitated in acetone overnight at -20 ºC and recovered by centrifugation at 17,000g for 20 minutes at 4 ºC. Protein pellets were resuspended in 8M Urea in Tris 10 mM [pH 8], reduced with 10 mM dithiothreitol at 50 °C for 30 min and alkylated with 50 mM iodoacetamide for 20 min at room temperature (RT) in the dark. Samples were digested for 4h at RT with Lys-C enzyme/substrate (Promega (V167), USA) (enzyme/substrate ratio 1:50), and then diluted four times with 50 mM ammonium bicarbonate for further trypsin digestion (Promega, USA) at 37 °C overnight (enzyme/substrate ratio 1:50). The digested peptides were desalted using a SepPak C18 cartridge and dried in a SpeedVac, prior to analysis by mass spectrometry (MS) using a label-free quantitative approach. Thus, peptide samples (approximately 500 ng/sample) were loaded onto a nano-ACQUITY UPLC System (Waters, USA) connected on-line to an LTQ Orbitrap XL mass spectrometer (Thermo Electron, USA). An aliquot of each sample was loaded onto a Symmetry 300 C18 UPLC Trap column (180 µm x 20 mm, 5 µm: Waters), and the pre-column was connected to a BEH130 C18 column (75 µm x 200 mm, 1.7 µm: Waters, USA) and equilibrated in 3% acetonitrile and 0.1% formic acid. Peptides were eluted directly into an LTQ Orbitrap XL mass spectrometer (Thermo Finnigan, USA) through a nanoelectrospray capillary source (Proxeon Biosystems, Denmark) at 300 nl/min and using a 120 min linear gradient of 3–50% acetonitrile. The mass spectrometer automatically switched between MS and MS/MS acquisition in data-dependent acquisition mode. Full MS scan survey spectra (m/z 400–2000) were acquired in the orbitrap with mass resolution of 30,000 at m/z 400. After each survey scan, the six most intense ions above 1,000 counts were sequentially subjected to collision-induced dissociation (CID) in the linear ion trap. Precursors with charge states of 2 and 3 were selected specifically for CID and peptides were excluded from further analysis over 60 s using the dynamic exclusion feature.

A Progenesis LC-MS (Waters, USA) apparatus was used for the label-free analysis of differential protein expression. One run was used as a reference, to which the precursor masses in all the other samples were

aligned. Only features comprising charges of 2+ and 3+ were selected, and the raw abundances of each feature were normalized automatically and converted to logarithms against the reference run. A peak list containing the information of all the features was generated and exported to the Mascot search engine (Matrix Science Ltd., UK). Differentially expressed proteins were defined as follows: p-value (t-test) <0.05 and fold-change rates > 1.5 for up-regulated or <0.6 for down-regulated proteins identified in at least two replicates. Together with the fold change, the data were finally uploaded into the Ingenuity® Pathway Analysis (IPA) software (Ingenuity Systems, USA) to investigate their molecular and biological functions.

**2.6. Immunocytochemistry**

Cells were plated on 13 mm round glass coverslips and incubated at 37 ºC in 5% $CO_2$ prior to fixation for immunofluorescence, performing all experiments in triplicate: 1 x $10^4$ cells/coverslip plated when cultures were maintained for 24 hours; 2 x $10^3$ cells/coverslip when they were maintained for 5 days; and 2 x $10^4$ cells/coverslip were plated when they were maintained for 7 days. The cells were fixed with 4% paraformaldehyde (PFA: Sigma-Aldrich Chemicals, Spain) in PBS for 20 minutes and after washing in PBS, the cells were incubated for 1 hour at RT in blocking solution: 10% Bovine Serum Albumin (BSA: Sigma, Spain); 0.25% Triton-X 100; and 1% FBS in PBS. The cells were then incubated overnight at 4 ºC with the primary antibodies. Neuronal microtubules were stained with mouse anti-β-III-Tubulin (1:1,000 dilution: ThermoFisher (MA1-118), USA) and anti-GAP43 (1:1,000 dilution: Abcam (ab16053), UK), mesenchymal stem cell progenitors were stained with CD105 (1:100 dilution: Sigma-Aldrich Chemicals (HPA011862), Spain), while neural progenitors were stained with anti-Nestin (1:200 dilution: ThermoFisher (PA5-32517), USA), anti-GFAP (1:3,000 dilution: DAKO (Z0334), USA) and anti-NeuN (1:500 dilution: ThermoFisher (702022), USA), a specific marker for neurons. When anti-Ki67 was used, the cells were permeabilized with 0.2% Triton-X 100 in PBS for 25 minutes and then incubated for 20 minutes in blocking solution containing 4% FBS. The cells were incubated overnight at 4 ºC with anti-Ki67 (1:100 dilution: ThermoFisher, USA) in a buffer containing 0.03% Triton-X 100 and 3% BSA in PBS. The cells were incubated with the secondary antibodies for 1h at RT: AlexaFluor488 donkey anti-Rabbit (1:1000 dilution: Invitrogen (A21206), USA) and AlexaFluor568 donkey anti-Mouse (1:1000 dilution: Invitrogen (A10037), USA). The nuclei were stained with 4′, 6′-diamidino-2-phenylindole dihydrochloride (DAPI, 1:5,000 dilution: Panreac Applichem (A4099), Spain) and all the coverslips were then mounted with Fluoro-Gel medium (Electron Microscopy Sciences, USA). Images were acquired on an MMI CellCut plus (Olympus, Japan).

**2.7. Cell size and shape measurement**

Neuronal microtubules were identified by β-III-tubulin immunostaining, as described above and in triplicate cultures for each sample. A total of 100 cells were assessed per subject from 15 random microscopy fields. The area and perimeter occupied by microtubules was defined and measured with the ImageJ software (USA). The formula used to assess roundness was: $(perimeter^2)/(4*pi*area)$. A roundness value of 1.0 indicates a perfect circle, and higher values indicate oblong and non-circular objects [18].

**2.8. Focal adhesion immunolabelling**

To analyse focal adhesion, 2 x $10^3$ cells were plated were plated on a coverslip as indicated in the datasheet for the "actin cytoskeleton and focal adhesion staining kit" (Merck (FAK100), Spain). Cells were permeabilized with 0.5% Triton-X 100 in PBS for 30 minutes and then incubated in blocking solution for 1 hour at RT, containing 1% BSA. The primary anti-vinculin antibody (1:500 dilution: Merck (90227), Spain) was applied overnight (4 ºC) and after washing (5 minutes) in three times, the cells were incubated for 1h at RT with TRITC-conjugated Phalloidin (1:1000, Merck (90228), Spain) and an AlexaFluor488 Donkey anti-Mouse secondary antibody (1:1,000 dilution; ThermoFisher (A21202), USA). Images were acquired with an MMI CellCut plus (Olympus, Japan).

To quantify focal adhesions immunolabelled with anti-vinculin, images were analysed with ImageJ software (USA) and the total number of vinculin adhesion points were quantified per cell. The cell cultures were performed in triplicate and a total of 10 cells per sample were analysed.

**2.9. Western blot**

The extraction of total protein was performed by lysing the cells in Lysis buffer: 1% NP40, 50 mM HEPES [pH 7], 150 mM NaCl, 1 mM EDTA, supplemented with protease inhibitors. The protein samples (20 μg per well) were resolved by electrophoresis in TGX Stain Free Precast gels (Bio-Rad, Spain), each sample run in triplicate, and UV trans-illumination (1 min) images were obtained to control for loading (Bio-Rad ChemiDoc MP Imaging System, Spain). The proteins were then transferred to a PVDF membrane and after blocking for 30 min in 5% BSA, the membranes were probed overnight at 4 ºC with a mouse anti-β-actin antibody (1:200,000 dilution: Sigma (A1978), Japan). The membranes were washed thrice with 0.01% Triton-X 100 in PBS and incubated for 1 hour with the secondary antibody (1:10,000 dilution: ThermoFisher 926-32210, Spain). After washing, images were obtained on an Odyssey CLx Infrared Imaging System (Li-Cor, USA) and the protein bands were quantified with ImageJ software (USA). The β-actin levels were normalized to the total protein level.

**2.10. Adhesion assay**

Cells (1 x $10^4$ cells/coverslip) were plated on 13 mm round glass coverslips and incubated for 1 hour at 37 ºC in 5% $CO_2$ prior to fixation, each sample was studied in triplicate. The cells were then washed with PBS and fixed for 20 min with 4% PFA (Sigma, USA) in PBS. The nuclei were stained with DAPI (1:5,000 dilution, Panreac Applichem A4099, Spain) and all the coverslips were mounted with Fluoro-Gel medium (Electron Microscopy Sciences, USA). The images were acquired on an Olympus BX40 microscope equipped with an Olympus DP73 camera (Spain) at 20X and the total number of cells attached to the coverslips was quantified.

**2.11. Wound healing assay**

The assay was performed as indicated in the datasheet for the "Wound Healing Assay" (Ibidi, Germany). A 70 μl suspension of a 3 x $10^5$ cells was added into each well of the *2 Well Culture-Insert* and after 24 hours, when the cell monolayer was confluent, the *2* Well *Culture-Insert* was removed and fresh medium

was added. At this point (0 hours) a wound was made in the culture, which was free of cells, and images were then taken at 0, 24 and 48 hours in order to quantify the number of cells migrating into the wound and the percentage closure. Each sample was studied in triplicate.

**2.12. Apoptosis assay**

Apoptosis was evaluated by flow cytometry by measuring the levels of Annexin V (A) and Propidium Iodide (PI). Briefly, cells (2 x $10^4$ cells/well) were seeded in 6-well plates and incubated with Dulbecco's Modified Eagle Medium/Ham F-12 (DMEM/F12) containing 10% Foetal Bovine Serum (FBS), 2% GlutaMAX 100X and 1% antibiotic-antimycotic (Thermo Scientific, Spain) for 24 h, at 37 ºC, 5%$CO_2$. ON cells were detached with 0.25% trypsin-EDTA (GibcoBRL, USA), and incubated with anti-Annexin V (PB-V450, #560506, BD) and PI (#556463, BD) at 4ºC, 30 min. Fluorescence was measured with a Cytoflex cytometer (Beckman Coulter) and the CytoExpert software. Finally, data were analysed with FlowJo v 10.4 software.

**2.13. Statistical analysis**

For the demographic and clinical categorical data (gender and tobacco use), the differences between the controls and cannabis users were assessed with a two-tailed chi-squared test. Protein-related statistics were obtained with Progenesis LC-MS (Waters, USA) and the IPA software (QIAGEN, Germany) while functional-related statistical analysis was performed with GraphPad Prism 5 software (GraphPad Software, USA). For functional assays, the difference between the control and cannabis users was assessed using the Student´s t-test (unpaired, two-tailed) after a normal distribution was evaluated with a Kolmogorov-Smirnov test. Correlations were performed using a Pearson's test to evaluate the association between every neuropsychological test score, and the THC-COOH and 11-OH-THC plasma levels. The data were presented as means ± SEM and the differences were considered statistically significant at a p value $< 0.05$.

## 3. RESULTS

### 3.1. There are no differences in the demographic or clinical characteristics of cannabis users

When the demographic and clinical data of all the subjects was assessed (Table 1), no significant differences were observed between the control subjects and the cannabis users in terms of age, sex, weight, height, body mass index, tobacco and alcohol use or clinical assessment (premorbid intelligence quotient (IQ) and depressive symptoms).

### 3.2. Cannabis users show worse attentional performance

THC and its metabolites were measured in plasma. THC concentrations were undetectable in control subjects and cannabis users. The metabolites of THC were not detected in the control subjects (n = 7), whereas among the cannabis users (n = 6), plasma 11-OH-THC was found in 5 out of 6 subjects (mean concentration: 1.68 ± 0.55 ng/ml) and THC-COOH was detected in all of these subjects (29.76 ± 6.15 ng/ml). The neuropsychological assessment (Fig. 1) revealed that cannabis users exhibited significantly worse attentional performance than healthy controls in the spatial span direct recall test ($p<0.01$, Fig. 1A), consistent with previous data [11]. Furthermore, a trend towards worse working memory was also detected in the spatial span inverse recall test ($p=0.068$, Fig. 1D).

### 3.3. Fewer undifferentiated ON cells were obtained from cannabis users

Under proliferative conditions, the markers $CD105^+$, $Nestin^+$, $GFAP^+$, $\beta$-III-$Tubulin^+$ and $GAP43^+$ were detected in ON cells derived from control subjects 24 h post seeding (Fig. 2), reflecting the presence of mesenchymal cells (CD105), undifferentiated neural progenitors (Nestin), glial-like cells (GFAP) and immature neurons (β-III-Tubulin and GAP43), as described previously [7, 19, 20] A high proportion of cells (60-80%) were $Nestin^+$ and/or β-III-$Tubulin^+$, indicating their neural lineage (Fig. 2D-F, J-L) [21], yet no cells were positive for the multipotent stem cell marker, Sox2 (data not shown). Among the ON cells from cannabis users there was a significant decrease in the number of cells expressing the CD105 and GFAP markers ($t = 2.887$, $p = 0.0203$ and $t = 3.584$, $p = 0.0071$ respectively, Fig. 2C, I), and an increase in the $Nestin^+$ cells ($t = 2.318$, $p = 0.0491$, Fig. 2F). No changes were observed in the percentage of β-III-Tubulin or $GAP43^+$ cells ($t = 0.1724$, $p = 0.8674$ and $t = 0.3198$, $p = 0.7573$ respectively, Fig. 2L, O).

### 3.4. ON cells from cannabis users show proteomic alterations

The label free proteomic approach used identified 65 proteins that were differentially expressed between ON cells derived from control subjects and cannabis users (51 upregulated and 14 downregulated). By analysing the list of differentially expressed proteins with IPA, we obtained information about the alterations induced in canonical pathways, the molecular/cellular functions, the development of physiological systems, and related diseases and disorders (Figs. 3-4). We observed interesting effects on canonical pathways in cannabis users, including Integrin, ILK, FAK and Actin Cytoskeleton signalling, as well as on cell behavior like Fc Receptor-mediated phagocytosis, microtubule dynamics and its influence on cell morphology, cell development, and at the level of tissue assembly and organization. In addition, the changes affected cell growth and proliferation, and inhibited cell death (Fig. 4B-C). These pathways and activities are of interest because they play an important role in nervous system development and

function [22], proliferation and cell growth: [23]; apoptosis: [24]. Indeed, 19 proteins involved in nervous system development and activity were differentially expressed in ON cells from cannabis users (Fig. 3B), alterations to which has also been described in mental disorders and brain (neurological) pathologies [22, 25, 26, 27, 28, 29]. Indeed, some of the differentially expressed proteins identified were related to disorders like schizophrenia, DiGeorge syndrome, epilepsy or bipolar disorder (Fig. 4D). Complete and detailed information regarding the changes in the proteins can be found in the Supplementary Table 1.

Overall, according to IPA the proteins altered in ON cells from cannabis consumers were apparently involved in pathways related to cell viability, morphology and more importantly, neuronal development and function.

**3.5. ON cells from cannabis users have a distinct morphology**

Taking into account the proteomic results, we evaluated the potential changes in cell morphology by measuring the area and perimeter occupied by microtubules stained with β-III-Tubulin, as well as the cell shape (Fig. 5). After measuring 100 cells in each sample, there was an increase in size of the cells obtained from cannabis users relative to the controls ($t=7.804$, $p<0.0001$, Fig. 5B-D). Furthermore, a high percentage of cells had a roundness value between 2 and 4, with significant differences between groups in this parameter ($t = 2.804$, $p = 0.021$, Fig. 5E). These changes in cell morphology might be explained by the alterations in the proteomic assay, with an up-regulation of proteins related to actin cytoskeleton signalling (Fig. 3A). Moreover, we observed an increase in the β-Actin in cells derived from cannabis users when measured in western blots ($t=3.254$, $p=0.031$, Fig. 5F-G). Together, these data indicate that the cytoskeleton was altered in cells derived from cannabis users, with consequences for cell size and shape.

**3.6. Cannabis reduced adhesion while it did not modify migration**

In cell adhesion experiments, there were no initial differences in the number of dead cells, with 99.9% viability in both the experimental groups when assessed by trypan blue exclusion (data not shown). However, we did observe a decrease in the total number of attached ON cells derived from cannabis users, indicating a weaker adhesive capacity ($t= 2.730$, $p = 0.0293$, 3 replicates/cell line, Fig. 5H-J). We also quantified the number of focal adhesions in monolayer cultures of cells immunolabelled with anti-vinculin (Fig. 5K-L) and there were fewer focal adhesions in cells derived from cannabis users ($t = 3.859$, $p = 0.0048$, Fig. 5M). Whether the decrease in adhesion was related to an increase in cell migration was determined in a “scratch wound” assay, yet there were no differences in the migration rate of cells from control subjects and cannabis users (percentage closure: $t=0.4176$, $p=0.6872$; number of cells: $t=0.4619$, $p=0.6565$, Fig. 5N-P). Nevertheless, the proteomic analysis identified differentially expression of several proteins related to cell migration.

**3.7. Cannabis affects cell proliferation and viability but not cell differentiation**

Cell proliferation was evaluated by immunostaining cells for the specific Ki67 marker (Fig. 6D-E) and there was an increase in the number of proliferative ON cells from cannabis users relative to the controls ($t = 4.212$, $p = 0.0029$, Fig. 6B). This increase was consistent with the proteomic analysis in which there was an up-regulation of cell growth and proliferation proteins in cells from cannabis users (Fig. 4C) and proteins involved in cell cycle regulation (Supplementary Fig. 1). Despite the increase in proliferation, the total number of cells in culture was no different between the two groups ($t = 0.393$, $p = 0.704$, Fig. 6C).

To evaluate whether the changes in cell proliferation may affect differentiation, the expression of the NeuN neuronal marker and the GFAP astrocyte marker was assessed (Fig. 6G-J). After 7 days in culture, 40.22% of the cells were $NeuN^+$ in both groups, whereas no $GFAP^+$ cells were detected, indicating a high degree of mature cells expressing a neuronal, but not a glial marker. However, no differences were observed between groups in $NeuN^+$ labelling ($t = 0.0889$ $p = 0.9313$, Fig. 6F).

Finally, proteomic results indicated a potential down-regulation of cell death, based on the differential expression of the proteins identified (Fig. 4B). We observed a significant decrease in the proportion of Annexin V+/PI- and Annexin V+/PI+ cells derived from cannabis users relative to the controls, indicating a decrease in both early and late apoptosis in ON cells from cannabis users ($t = 2.975$, $p = 0.0177$ and $t = 2.827$, $p = 0.0222$ respectively: Fig. 6K-O), consistent with the proteomic data.

## 4. DISCUSSION

We show here that ON cells derived from cannabis users suffer cytoskeleton alterations, decreased attachment, enhanced cell proliferation and reduced cell death. These behavioural alterations are accompanied by changes in the expression of proteins that have been associated with cancer, gastrointestinal disease and neurodevelopmental pathways [30-33]. Thus, the ON cell model provides relevant information regarding the effects of cannabis on the brain that may be related to neuropsychiatric disorders.

ON cells are morphologically undifferentiated after 24 h *in vitro*, and most of them (>90%) express an antigen associated with bone marrow stromal cells (CD105), as indicated previously [6]. Furthermore, 60-80% express the markers of neural progenitors (Nestin) and/or immature neurons (β-III-Tubulin and GAP43) [6, 11], corroborating their neural lineage. Moreover, around 20% of cells express GFAP, indicating the presence of astroglial-like cells previously described as neuroblasts in ON cell populations [34, 35]. Furthermore, multipotent stem cell marker, Sox2, expressed by ON [36] was not detected in our cell cultures. Although previous studies described the presence of Sox2 in multipotent stem cells in olfactory mucosa *in vivo* [20, 36] and in neurosphere cultures derived from ON stem cells [37] reports using adhered cultures do not show the presence of this transcription factor [20]. Cells adhered onto a substrate behave differently when compared with cells grown under floating conditions since they tend to differentiate losing stem cell properties such as the transcription factor Sox2. ON cells from cannabis users also expressed the same markers as control cells, although there were significantly fewer $CD105^+$ and $GFAP^+$ cells, and more $Nestin^+$ cells in these cultures. Nestin and GFAP are thought to be neural progenitor and stem cell markers, respectively [21, 34], suggesting that a compensatory mechanism is occurring in cannabis consumers, which might be boosting the production of $Nestin^+$ progenitors at the expense of depletion of the stem cell pool ($GFAP^+$ glial-like cells). Thus, the change we observed in the number of $Nestin^+$ and $GFAP^+$ cells could be explained by alterations in cell growth and differentiation. Likewise, a decrease in CD105 is associated with the differentiation of mesenchymal stem cells derived from different tissues [38-40]. By contrast, we did not observe a change in the number of immature β-III-$Tubulin^+$ and $GAP43^+$ cells after 24 h *in vitro*, nor in the number of $NeuN^+$ cells after 7 days *in vitro*, indicating that the changes in the number of neuronal progenitors present in the ON of cannabis users do not necessarily lead to ON cell differentiation.

We evaluated the proteomic profile of ON cells after 5 days *in vitro*, identifying 49 upregulated proteins and 16 downregulated proteins in the cells from cannabis users as compared to cells from healthy controls. Several proteins involved in the actin cytoskeleton signaling pathway, and in the Integrin and ILK signaling pathways, were significantly affected in ON cells from cannabis users. ILK fulfils an essential role in connecting the cytoplasmic tail of integrin β subunits to the actin cytoskeleton and in regulating actin polymerization. These proteomic data were in agreement with changes in cell morphology that was assessed by measuring the size and shape of β-III-Tubulin stained cells. In control ON cells, microtubules form an extensive and compact network that appears to originate from the

microtubule organizing centre located close to the nucleus. There was a robust increase in the size of β-III-Tubulin stained ON cells from cannabis users, with differences in roundness that suggests a reorganization of microtubules. Furthermore, changes in microtubule assembly were accompanied by stronger β-actin expression in ON cells from cannabis user that was evident in western blots, suggesting that two cytoskeletal structures may be significantly affected by cannabis, microtubules and microfilaments. The cytoskeleton is involved in a number of biological processes, ranging from those that involve the maintenance of cell shape to those affecting cell proliferation and other activities [41-43]. The mechanisms by which cannabis alters cytoskeletal architecture are unknown, although THC was shown to influence the assembly and disassembly of tubulin *in vitro* [44]. Since the cytoskeleton is closely associated with cell membranes, the interaction of cannabis with the lipid bilayer or membrane bound enzyme systems may adversely affect the architecture of the cytoskeleton. In this sense, a recent study using SR-FTIR spectroscopy found that intracellular lipid chains are disordered in ON cells from cannabis users, the membrane displaying an altered lipid composition with a higher rate of membrane lipid renewal and peroxidation, and more proteins with β-sheet structures [12]. Thus, these data strongly support the increased cell size and cytoskeletal alteration in the ON cells of cannabis users. Interestingly, earlier data showed that ON cells from bipolar patients were larger and displayed cytoskeletal alterations [9].

Cannabis may also affect the cytoskeleton indirectly through its effects on other cell structures or biochemical activities. Indeed, cytoskeletal abnormalities may be related to other cell functions like cell adhesion and migration. ACTG1, DOCK1 and RAP1B also belong to FAK signalling and Paxillin pathways (Figure 3 and 4). Paxillin is a focal adhesion-associated phosphotyrosine-containing protein. The proteomic alterations to these pathways suggest there are changes at the cell surface of ON cells from cannabis users, as demonstrated by the weaker vinculin staining in ON cells from cannabis users and the decrease in the total number of attached cells when adhesion was evaluated. Interestingly, schizophrenic ON cells have half the size and number of focal adhesion [45, 10, 46], and as focal adhesions are related to cell attachment, detachment and migration [46], we evaluated the motility of these cells. While no changes in cell migration were detected, there were differences in the expression of proteins involved in migration (CD9, DOCK1, FERMT2, RAP1B, CAPZB, RAB35, ARPC2, SLC2A1, SYNE1, SYNE2, MGLL and CALD1). Many of these proteins are not exclusively involved in migration, which could explain why the alterations in their expression did not affect migration (e.g. DOCK1 or RAP1B are also involved in actin cytoskeletal signaling). Hence, the effects of cannabis use on ON cell migration should be studied further, for example assessing the migration of these cells in response to different extracellular matrix factors [46].

In terms of cell proliferation, ON cells from cannabis users had a higher rate of proliferation when evaluated with the Ki67 marker. However, cell differentiation was not affected, as the number of $NeuN^+$ neurons and $GFAP^+$ astrocytes did not change, even though the proteomic analysis suggested alterations in neural proliferation and axon guidance. In this sense, the STMN2 (stathmin-2) protein is particularly relevant as it is involved in axon guidance and the Endocannabinoid Developing Neuron pathway, and the

down-regulation seen for in STMN2 was consistent with the low levels detected in the human brains exposed to THC [47]. By reducing STMN2, THC favours ectopic filopodia formation and it alters axon morphology [47]. Furthermore, ON cells from cannabis users underwent less apoptosis, both early (Annexin V+/PI-) and late apoptosis (Annexin V+/PI+). Indeed, several proteins related to cell death were differentially expressed in ON cells from cannabis users. If these alterations were to occur in the foetal or young brain, they would alter the timing and balance of neuronal birth, differentiation and death, consequently affecting the timing and success of synaptic connectivity. Such changes would produce fundamental differences in brain function, as reported in chronic cannabis users [48-49]. In fact, chronic cannabis appeared to directly affect cognitive function, specifically decreasing attentional performance in our study. Furthermore, attention and working memory impairments have been found in larger cohorts of cannabis users [11]

Interestingly, increased cell proliferation and reduced cell adhesion was evident in olfactory cultures from individuals with schizophrenia, although no alterations to apoptosis were detected [7, 8]. Thus, it is likely that cannabis might predispose or precipitate alterations leading to other psychiatric diseases. Accordingly, the proteomic analysis identified protein alterations common to cannabis and schizophrenic patients, such as those in EWSR1, RAB32 and STMN2 ([25, 26]. Indeed, EWSR1 was altered in the same direction in post-mortem superior temporal gyrus tissue and in peripheral blood lymphocytes from individuals with schizophrenia [26]. Monoglyceride lipase (MGLL-1) metabolizes the endogenous cannabinoid 2-arachidonoylglycerol and ON cells from cannabis users express this protein this protein weaklier, while 2-arachidonylglycerol metabolism is enhanced in the prefrontal cortex of subjects with schizophrenia [29]. Overall, these data show similarities between data from ON cells derived from cannabis users and previous findings from schizophrenia patients.

In addition to schizophrenia, the proteomic analysis revealed a reduction in *TBX1* (T-box containing transcription factor) expression in ON cells from cannabis users. Haplo-insufficiency of *TBX1* is thought to contribute significantly to the cardiovascular, endocrine and neurogenic phenotypes of DiGeorge Syndrome (DGS, 22q11.2 deletion syndrome -22q11DS) and Velo-Cardio-Facial Syndrome [50, 51]. Indeed, approximately 23-30% of late adolescents and young adults with DGS develop psychotic symptoms. Moreover, the *TBX1* gene has been involved in the pathogenesis of schizophrenia in some patients [52]. In animal models, congenic *TBX1* heterozygous mice display autism-related behavioural phenotypes [53, 54]. Mutations and haplo-insufficiency of the *TBX1* gene are sufficient to cause reduced pre-pulse inhibition, a behavioural abnormality that is associated with a schizophrenic endophenotype [55]

ON cells from patients with bipolar disease and from cannabis users share some characteristics. Indeed, ON cells from bipolar patients are also larger and have an altered cytoskeleton [9], similar to the changes found in ON cells from cannabis users. Moreover, our proteomic analysis detected a down-regulation of SYNE1 (nesprin-1), and polymorphisms of this gene have been associated with susceptibility to bipolar and unipolar mood disorders [28]. Apart from mental disorders, proteins differentially expressed in our

samples are also related to other neurological disorders, such as epilepsy [56], Glut1 syndrome [57], Charcot-Marie-Tooth disease [58], deafness [59], spinocerebellar ataxia [60], microcephaly/epilepsy/diabetes syndrome [61] and episodic choreoathetosis/spasticity [62].

In summary, our data, in a small sample of cannabis users, show that ON cells derived from cannabis users exhibit changes in cell morphology, weaker adhesion, and alterations to their cell cycle, cell growth and proliferation, although we did not observe any effects on differentiation. These changes could be related to alterations in cytoskeletal proteins and signalling pathways. All these cellular processes are important for brain development, maintenance and function. These alterations can be caused by local or systemic effect of cannabis because it is consumed smoked. Importantly, our biochemical analyses show that the dose of cannabis used was able to significantly increase plasma concentrations of THC metabolites. Therefore, this dose (5 or more cannabis cigarettes per day) appears to be the desired dose of THC for ON alterations. In addition, in previous studies using this cohort of cannabis users, we have shown relevant changes in CB1-5-HT2A receptor heteromer expression in ON cells as compared to healthy controls (Galindo et al., 2018). Further studies with larger cohorts should be carried out to control for the effects of sex, age, history of consumption of cannabis or other substances (tobacco and alcohol), and to correlate the changes produced by cannabis with the level of use/abuse. Finally, it is important to note that some of these alterations have been described in ON cells of schizophrenia and bipolar patients, providing a possible link between cannabis consumption and the risk of suffering a psychiatric disorder.

**Acknowledgements:** We would like to thank Dr. Antonia Díaz Gañete for her excellent assistance at the beginning of this project, the CIC-Biogune Proteomics platform, especially Dr. Ibon Iloro and Dr. Felix Elortza for their technical assistance. Network images were obtained with IPA, thanks to the assistance provided by the PAB (Andalusian Bioinformatics Platform) center, University of Malaga. We would like to acknowledge the Clinical Research Unit at the IMIM-Hospital del Mar Research Institute for their expertise in nasal brushing, especially to Marta Pérez Otero and Dr. Ana M. Aldea Perona, and to Dr. Aida Cuenca-Royo for the neuropsychological evaluation. This study was supported by grants co-financed by the "Fondo Europeo de Desarrollo Regional" (FEDER)-UE "A way to build Europe" from the "Programa Operativo de Andalucía FEDER, Iniciativa Territorial Integrada ITI 2014-2020 Consejería Salud, Junta de Andalucía" (PI-0009-2017); the "Consejería de Economía, Innovación, Ciencia y Empleo de la Junta de Andalucía" (CTS-510); Plan Nacional sobre Drogas (2019I041), the "Ministerio de Economía, Industria y Competitividad ("Juan de la Cierva Incorporación" postdoctoral grant IJCI-2015-23280), the "Centro de Investigación Biomédica en Red de Salud Mental-CIBERSAM" (CB/07/09/0033; CB/07/09/0029), and Instituto de Salud Carlos III, Ministerio de Ciencia e Innovación de España y fondos FEDER (PI18/00053 to P.R.).

## 5. REFERENCES


1. Campeny E, Lopez-Pelayo H, Nutt D, Blithikioti C, Oliveras C, Nuno L, Maldonado R, Florez G, Arias F, Fernandez-Artamendi S, Villalbi JR, Sellares J, Ballbe M, Rehm J, Balcells-Olivero MM, Gual A (2020) The blind men and the elephant: Systematic review of systematic reviews of cannabis use related health harms. Eur Neuropsychopharmacol 33:1-35. doi:10.1016/j.euroneuro.2020.02.003

2. Maccarrone M, Maldonado R, Casas M, Henze T, Centonze D (2017) Cannabinoids therapeutic use: what is our current understanding following the introduction of THC, THC:CBD oromucosal spray and others? Expert Rev Clin Pharmacol 10 (4):443-455. doi:10.1080/17512433.2017.1292849

3. Bloomfield MAP, Hindocha C, Green SF, Wall MB, Lees R, Petrilli K, Costello H, Ogunbiyi MO, Bossong MG, Freeman TP (2019) The neuropsychopharmacology of cannabis: A review of human imaging studies. Pharmacol Ther 195:132-161. doi:10.1016/j.pharmthera.2018.10.006

4. Szutorisz H, Hurd YL (2016) Epigenetic Effects of Cannabis Exposure. Biol Psychiatry 79 (7):586-594. doi:10.1016/j.biopsych.2015.09.014

5. Leung CT, Coulombe PA, Reed RR (2007) Contribution of olfactory neural stem cells to tissue maintenance and regeneration. Nat Neurosci 10 (6):720-726. doi:10.1038/nn1882

6. Matigian N, Abrahamsen G, Sutharsan R, Cook AL, Vitale AM, Nouwens A, Bellette B, An J, Anderson M, Beckhouse AG, Bennebroek M, Cecil R, Chalk AM, Cochrane J, Fan Y, Feron F, McCurdy R, McGrath JJ, Murrell W, Perry C, Raju J, Ravishankar S, Silburn PA, Sutherland GT, Mahler S, Mellick GD, Wood SA, Sue CM, Wells CA, Mackay-Sim A (2010) Disease-specific, neurosphere-derived cells as models for brain disorders. Dis Model Mech 3 (11-12):785-798. doi:10.1242/dmm.005447

7. Feron F, Perry C, Hirning MH, McGrath J, Mackay-Sim A (1999) Altered adhesion, proliferation and death in neural cultures from adults with schizophrenia. Schizophr Res 40 (3):211-218. doi:10.1016/s0920-9964(99)00055-9

8. McCurdy RD, Feron F, Perry C, Chant DC, McLean D, Matigian N, Hayward NK, McGrath JJ, Mackay-Sim A (2006) Cell cycle alterations in biopsied olfactory neuroepithelium in schizophrenia and bipolar I disorder using cell culture and gene expression analyses. Schizophr Res 82 (2-3):163-173. doi:10.1016/j.schres.2005.10.012

9. Solis-Chagoyan H, Calixto E, Figueroa A, Montano LM, Berlanga C, Rodriguez-Verdugo MS, Romo F, Jimenez M, Gurrola CZ, Riquelme A, Benitez-King G (2013) Microtubule organization and L-type voltage-activated calcium current in olfactory neuronal cells obtained from patients with schizophrenia and bipolar disorder. Schizophr Res 143 (2-3):384-389. doi:10.1016/j.schres.2012.11.035

10. Munoz-Estrada J, Benitez-King G, Berlanga C, Meza I (2015) Altered subcellular distribution of the 75-kDa DISC1 isoform, cAMP accumulation, and decreased neuronal migration in schizophrenia and bipolar disorder: implications for neurodevelopment. CNS Neurosci Ther 21 (5):446-453. doi:10.1111/cns.12377

11. Galindo L, Moreno E, Lopez-Armenta F, Guinart D, Cuenca-Royo A, Izquierdo-Serra M, Xicota L, Fernandez C, Menoyo E, Fernandez-Fernandez JM, Benitez-King G, Canela EI, Casado V, Perez V, de la Torre R, Robledo P (2018) Cannabis Users Show Enhanced Expression of CB1-5HT2A Receptor Heteromers in Olfactory Neuroepithelium Cells. Mol Neurobiol 55 (8):6347-6361. doi:10.1007/s12035-017-0833-7

12. Saladrigas-Manjon S, Ducic T, Galindo L, Fernandez-Aviles C, Perez V, de la Torre R, Robledo P (2020) Effects of Cannabis Use on the Protein and Lipid Profile of Olfactory Neuroepithelium Cells from Schizophrenia Patients Studied by Synchrotron-Based FTIR Spectroscopy. Biomolecules 10 (2). doi:10.3390/biom10020329

13. Buchanan JT, Grillner S, Cullheim S, Risling M (1989) Identification of excitatory interneurons contributing to generation of locomotion in lamprey: structure, pharmacology, and function. J Neurophysiol 62 (1):59-69. doi:10.1152/jn.1989.62.1.59

14. Endicott J, Spitzer RL, Fleiss JL, Cohen J (1976) The global assessment scale. A procedure for measuring overall severity of psychiatric disturbance. Arch Gen Psychiatry 33 (6):766-771. doi:10.1001/archpsyc.1976.01770060086012

15. Wechsler D (1997) Wechsler Adult Intelligence Scale. Third Edition edn.,

16. Benton AL (1983) Multilingual aplasia examination(2nd ed edn.,)

17. Zhang X (2016) Quantitative Analysis of THC and its Metabolites in Whole Blood Using LC-MS/MS for Toxicology and Forensic Laboratories. Waters, the science of what's possible,

18. DeCoster MA (2010) Microscopy and image analysis of individual and group cell shape changes during apoptosis Microscopy: Science, Technology, Applications and Education

19. Delorme B, Nivet E, Gaillard J, Haupl T, Ringe J, Deveze A, Magnan J, Sohier J, Khrestchatisky M, Roman FS, Charbord P, Sensebe L, Layrolle P, Feron F (2010) The human nose harbors a niche of olfactory ectomesenchymal stem cells displaying neurogenic and osteogenic properties. Stem Cells Dev 19 (6):853-866. doi:10.1089/scd.2009.0267

20. Borgmann-Winter K, Willard SL, Sinclair D, Mirza N, Turetsky B, Berretta S, Hahn CG (2015) Translational potential of olfactory mucosa for the study of neuropsychiatric illness. Transl Psychiatry 5:e527. doi:10.1038/tp.2014.141

21. Benitez-King G, Riquelme A, Ortiz-Lopez L, Berlanga C, Rodriguez-Verdugo MS, Romo F, Calixto E, Solis-Chagoyan H, Jimenez M, Montano LM, Ramirez-Rodriguez G, Morales-Mulia S, Dominguez-Alonso A (2011) A non-invasive method to isolate the neuronal linage from the nasal epithelium from schizophrenic and bipolar diseases. J Neurosci Methods 201 (1):35-45. doi:10.1016/j.jneumeth.2011.07.009

22. Benitez-King G, Valdes-Tovar M, Trueta C, Galvan-Arrieta T, Argueta J, Alarcon S, Lora-Castellanos A, Solis-Chagoyan H (2016) The microtubular cytoskeleton of olfactory neurons derived from patients with schizophrenia or with bipolar disorder: Implications for biomarker characterization, neuronal physiology and pharmacological screening. Mol Cell Neurosci 73:84-95. doi:10.1016/j.mcn.2016.01.013

23. Sacco R, Cacci E, Novarino G (2018) Neural stem cells in neuropsychiatric disorders. Curr Opin Neurobiol 48:131-138. doi:10.1016/j.conb.2017.12.005

24. Yamaguchi Y, Miura M (2015) Programmed cell death in neurodevelopment. Dev Cell 32 (4):478-490. doi:10.1016/j.devcel.2015.01.019

25. Hakak Y, Walker JR, Li C, Wong WH, Davis KL, Buxbaum JD, Haroutunian V, Fienberg AA (2001) Genome-wide expression analysis reveals dysregulation of myelination-related genes in chronic schizophrenia. Proc Natl Acad Sci U S A 98 (8):4746-4751. doi:10.1073/pnas.081071198

26. Bowden NA, Scott RJ, Tooney PA (2008) Altered gene expression in the superior temporal gyrus in schizophrenia. BMC Genomics 9:199. doi:10.1186/1471-2164-9-199

27. Morin M, Bryan KE, Mayo-Merino F, Goodyear R, Mencia A, Modamio-Hoybjor S, del Castillo I, Cabalka JM, Richardson G, Moreno F, Rubenstein PA, Moreno-Pelayo MA (2009) In vivo and in vitro effects of two novel gamma-actin (ACTG1) mutations that cause DFNA20/26 hearing impairment. Hum Mol Genet 18 (16):3075-3089. doi:10.1093/hmg/ddp249

28. Green EK, Grozeva D, Forty L, Gordon-Smith K, Russell E, Farmer A, Hamshere M, Jones IR, Jones L, McGuffin P, Moran JL, Purcell S, Sklar P, Owen MJ, O'Donovan MC, Craddock N (2013) Association at SYNE1 in both bipolar disorder and recurrent major depression. Mol Psychiatry 18 (5):614-617. doi:10.1038/mp.2012.48

29. Volk DW, Lewis DA (2016) The Role of Endocannabinoid Signaling in Cortical Inhibitory Neuron Dysfunction in Schizophrenia. Biol Psychiatry 79 (7):595-603. doi:10.1016/j.biopsych.2015.06.015

30. Prescot AP, Locatelli AE, Renshaw PF, Yurgelun-Todd DA (2011) Neurochemical alterations in adolescent chronic marijuana smokers: a proton MRS study. Neuroimage 57 (1):69-75. doi:10.1016/j.neuroimage.2011.02.044

31. Jacobus J, Tapert SF (2014) Effects of cannabis on the adolescent brain. Curr Pharm Des 20 (13):2186-2193. doi:10.2174/13816128113199990426

32. Gubatan J, Staller K, Barshop K, Kuo B (2016) Cannabis Abuse Is Increasing and Associated with Increased Emergency Department Utilization in Gastroenterology Patients. Dig Dis Sci 61 (7):1844-1852. doi:10.1007/s10620-016-4090-9

33. Ghasemiesfe M, Barrow B, Leonard S, Keyhani S, Korenstein D (2019) Association Between Marijuana Use and Risk of Cancer: A Systematic Review and Meta-analysis. JAMA Netw Open 2 (11):e1916318. doi:10.1001/jamanetworkopen.2019.16318

34. Wolozin B, Sunderland T, Zheng BB, Resau J, Dufy B, Barker J, Swerdlow R, Coon H (1992) Continuous culture of neuronal cells from adult human olfactory epithelium. J Mol Neurosci 3 (3):137-146. doi:10.1007/BF02919405

35. Hahn CG, Han LY, Rawson NE, Mirza N, Borgmann-Winter K, Lenox RH, Arnold SE (2005) In vivo and in vitro neurogenesis in human olfactory epithelium. J Comp Neurol 483 (2):154-163. doi:10.1002/cne.20424

36. Lin B, Coleman JH, Peterson JN, Zunitch MJ, Jang W, Herrick DB, Schwob JE (2017) Injury Induces Endogenous Reprogramming and Dedifferentiation of Neuronal Progenitors to Multipotency. Cell Stem Cell 21 (6):761-774 e765. doi:10.1016/j.stem.2017.09.008

37. Jimenez-Vaca AL, Benitez-King G, Ruiz V, Ramirez-Rodriguez GB, Hernandez-de la Cruz B, Salamanca-Gomez FA, Gonzalez-Marquez H, Ramirez-Sanchez I, Ortiz-Lopez L, Velez-Del Valle C, Ordonez-Razo RM (2018) Exfoliated Human Olfactory Neuroepithelium: A Source of Neural Progenitor Cells. Mol Neurobiol 55 (3):2516-2523. doi:10.1007/s12035-017-0500-z

38. Jin HJ, Park SK, Oh W, Yang YS, Kim SW, Choi SJ (2009) Down-regulation of CD105 is associated with multi-lineage differentiation in human umbilical cord blood-derived mesenchymal stem cells. Biochem Biophys Res Commun 381 (4):676-681. doi:10.1016/j.bbrc.2009.02.118

39. Alev C, McIntyre BA, Ota K, Sheng G (2010) Dynamic expression of Endoglin, a TGF-beta co-receptor, during pre-circulation vascular development in chick. Int J Dev Biol 54 (4):737-742. doi:10.1387/ijdb.092962ca

40. Noda S, Kawashima N, Yamamoto M, Hashimoto K, Nara K, Sekiya I, Okiji T (2019) Effect of cell culture density on dental pulp-derived mesenchymal stem cells with reference to osteogenic differentiation. Sci Rep 9 (1):5430. doi:10.1038/s41598-019-41741-w

41. Pedersen SF, Hoffmann EK, Mills JW (2001) The cytoskeleton and cell volume regulation. Comp Biochem Physiol A Mol Integr Physiol 130 (3):385-399. doi:10.1016/s1095-6433(01)00429-9

42. Fletcher DA, Mullins RD (2010) Cell mechanics and the cytoskeleton. Nature 463 (7280):485-492. doi:10.1038/nature08908

43. Kapitein LC, Hoogenraad CC (2015) Building the Neuronal Microtubule Cytoskeleton. Neuron 87 (3):492-506. doi:10.1016/j.neuron.2015.05.046

44. Tahir SK, Zimmerman AM (1991) Influence of marihuana on cellular structures and biochemical activities. Pharmacol Biochem Behav 40 (3):617-623. doi:10.1016/0091-3057(91)90372-9

45. Fan Y, Abrahamsen G, Mills R, Calderon CC, Tee JY, Leyton L, Murrell W, Cooper-White J, McGrath JJ, Mackay-Sim A (2013) Focal adhesion dynamics are altered in schizophrenia. Biol Psychiatry 74 (6):418-426. doi:10.1016/j.biopsych.2013.01.020

46. Tee JY, Sutharsan R, Fan Y, Mackay-Sim A (2017) Cell migration in schizophrenia: Patient-derived cells do not regulate motility in response to extracellular matrix. Mol Cell Neurosci 80:111-122. doi:10.1016/j.mcn.2017.03.005

47. Tortoriello G, Morris CV, Alpar A, Fuzik J, Shirran SL, Calvigioni D, Keimpema E, Botting CH, Reinecke K, Herdegen T, Courtney M, Hurd YL, Harkany T (2014) Miswiring the brain: Delta9-tetrahydrocannabinol disrupts cortical development by inducing an SCG10/stathmin-2 degradation pathway. EMBO J 33 (7):668-685. doi:10.1002/embj.201386035

48. Newman SD, Cheng H, Schnakenberg Martin A, Dydak U, Dharmadhikari S, Hetrick W, O'Donnell B (2019) An Investigation of Neurochemical Changes in Chronic Cannabis Users. Front Hum Neurosci 13:318. doi:10.3389/fnhum.2019.00318

49. Kim SH, Yang JW, Kim KH, Kim JU, Yook TH (2019) A Review on Studies of Marijuana for Alzheimer's Disease - Focusing on CBD, THC. J Pharmacopuncture 22 (4):225-230. doi:10.3831/KPI.2019.22.030

50. Lindsay EA, Vitelli F, Su H, Morishima M, Huynh T, Pramparo T, Jurecic V, Ogunrinu G, Sutherland HF, Scambler PJ, Bradley A, Baldini A (2001) Tbx1 haploinsufficieny in the DiGeorge syndrome region causes aortic arch defects in mice. Nature 410 (6824):97-101. doi:10.1038/35065105

51. Jonas RK, Montojo CA, Bearden CE (2014) The 22q11.2 deletion syndrome as a window into complex neuropsychiatric disorders over the lifespan. Biol Psychiatry 75 (5):351-360. doi:10.1016/j.biopsych.2013.07.019

52. Ping LY, Chuang YA, Hsu SH, Tsai HY, Cheng MC (2016) Screening for Mutations in the TBX1 Gene on Chromosome 22q11.2 in Schizophrenia. Genes (Basel) 7 (11). doi:10.3390/genes7110102

53. Hiramoto T, Kang G, Suzuki G, Satoh Y, Kucherlapati R, Watanabe Y, Hiroi N (2011) Tbx1: identification of a 22q11.2 gene as a risk factor for autism spectrum disorder in a mouse model. Hum Mol Genet 20 (24):4775-4785. doi:10.1093/hmg/ddr404

54. Takahashi T, Okabe S, Broin PO, Nishi A, Ye K, Beckert MV, Izumi T, Machida A, Kang G, Abe S, Pena JL, Golden A, Kikusui T, Hiroi N (2016) Structure and function of neonatal social communication in a genetic mouse model of autism. Mol Psychiatry 21 (9):1208-1214. doi:10.1038/mp.2015.190

55. Paylor R, Glaser B, Mupo A, Ataliotis P, Spencer C, Sobotka A, Sparks C, Choi CH, Oghalai J, Curran S, Murphy KC, Monks S, Williams N, O'Donovan MC, Owen MJ, Scambler PJ, Lindsay E (2006) Tbx1 haploinsufficiency is linked to behavioral disorders in mice and humans: implications for 22q11 deletion syndrome. Proc Natl Acad Sci U S A 103 (20):7729-7734. doi:10.1073/pnas.0600206103

56. Katona I (2015) Cannabis and Endocannabinoid Signaling in Epilepsy. Handb Exp Pharmacol 231:285-316. doi:10.1007/978-3-319-20825-1_10

57. Brockmann K (2009) The expanding phenotype of GLUT1-deficiency syndrome. Brain Dev 31 (7):545-552. doi:10.1016/j.braindev.2009.02.008

58. Alazami AM, Alzahrani F, Bohlega S, Alkuraya FS (2014) SET binding factor 1 (SBF1) mutation causes Charcot-Marie-tooth disease type 4B3. Neurology 82 (18):1665-1666. doi:10.1212/WNL.0000000000000331

59. Morin M, Bryan KE, Mayo-Merino F, Goodyear R, Mencia A, Modamio-Hoybjor S*, et al.* (2009). In vivo and in vitro effects of two novel gamma-actin (ACTG1) mutations that cause DFNA20/26 hearing impairment. Hum Mol Genet 18**:** 3075-3089.

60. Gros-Louis F, Dupre N, Dion P, Fox MA, Laurent S, Verreault S, Sanes JR, Bouchard JP, Rouleau GA (2007) Mutations in SYNE1 lead to a newly discovered form of autosomal recessive cerebellar ataxia. Nat Genet 39 (1):80-85. doi:10.1038/ng1927

61. Shalev SA, Tenenbaum-Rakover Y, Horovitz Y, Paz VP, Ye H, Carmody D, Highland HM, Boerwinkle E, Hanis CL, Muzny DM, Gibbs RA, Bell GI, Philipson LH, Greeley SA (2014) Microcephaly, epilepsy, and neonatal diabetes due to compound heterozygous mutations in IER3IP1: insights into the natural history of a rare disorder. Pediatr Diabetes 15 (3):252-256. doi:10.1111/pedi.12086

62. Weber YG, Lerche H (2009) Genetics of paroxysmal dyskinesias. Curr Neurol Neurosci Rep 9 (3):206-211. doi:10.1007/s11910-009-0031-8

**FIGURE 1**

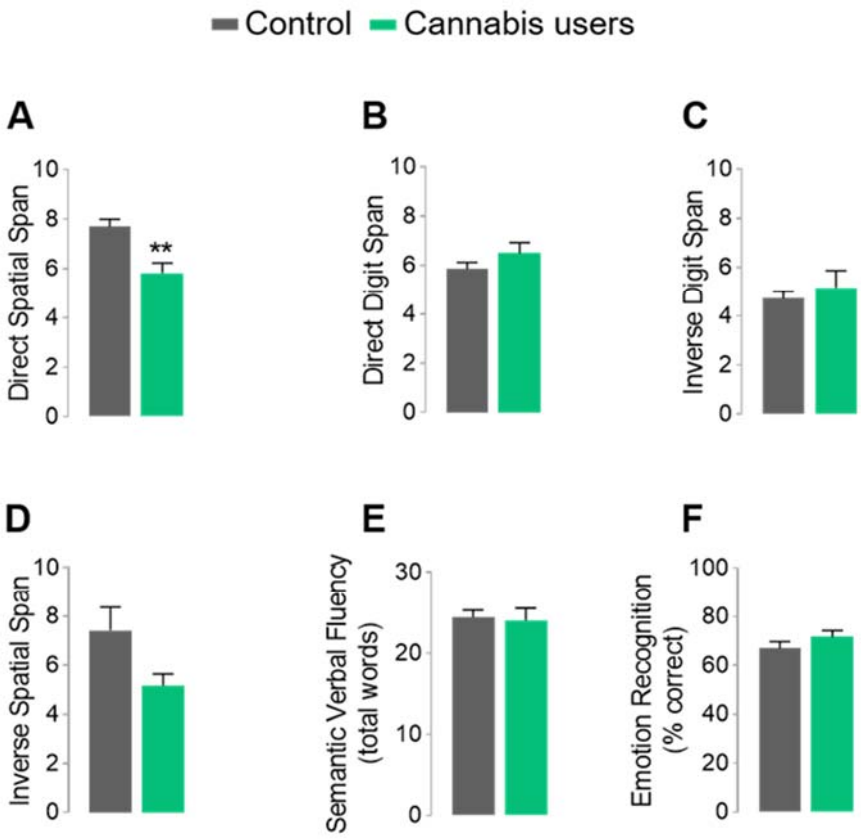


**Figure 1. Neuropsychological assessment.** A significant decrease in attention performance was observed in cannabis users when assessed by the direct spatial span test **(A)** but not the direct digit span test **(B)**. No significant differences between groups were observed in terms of working memory, assessed by the inverse digit span test **(C)** and the inverse spatial span test **(D)**. Executive functions were evaluated with the verbal fluency test **(E)**, and social and emotional cognition was assessed with the emotion recognition test **(F)**: * $p < 0,05$ (*Student's t-test*: Control subjects n = 7, Cannabis users n = 6).

**FIGURE 2**

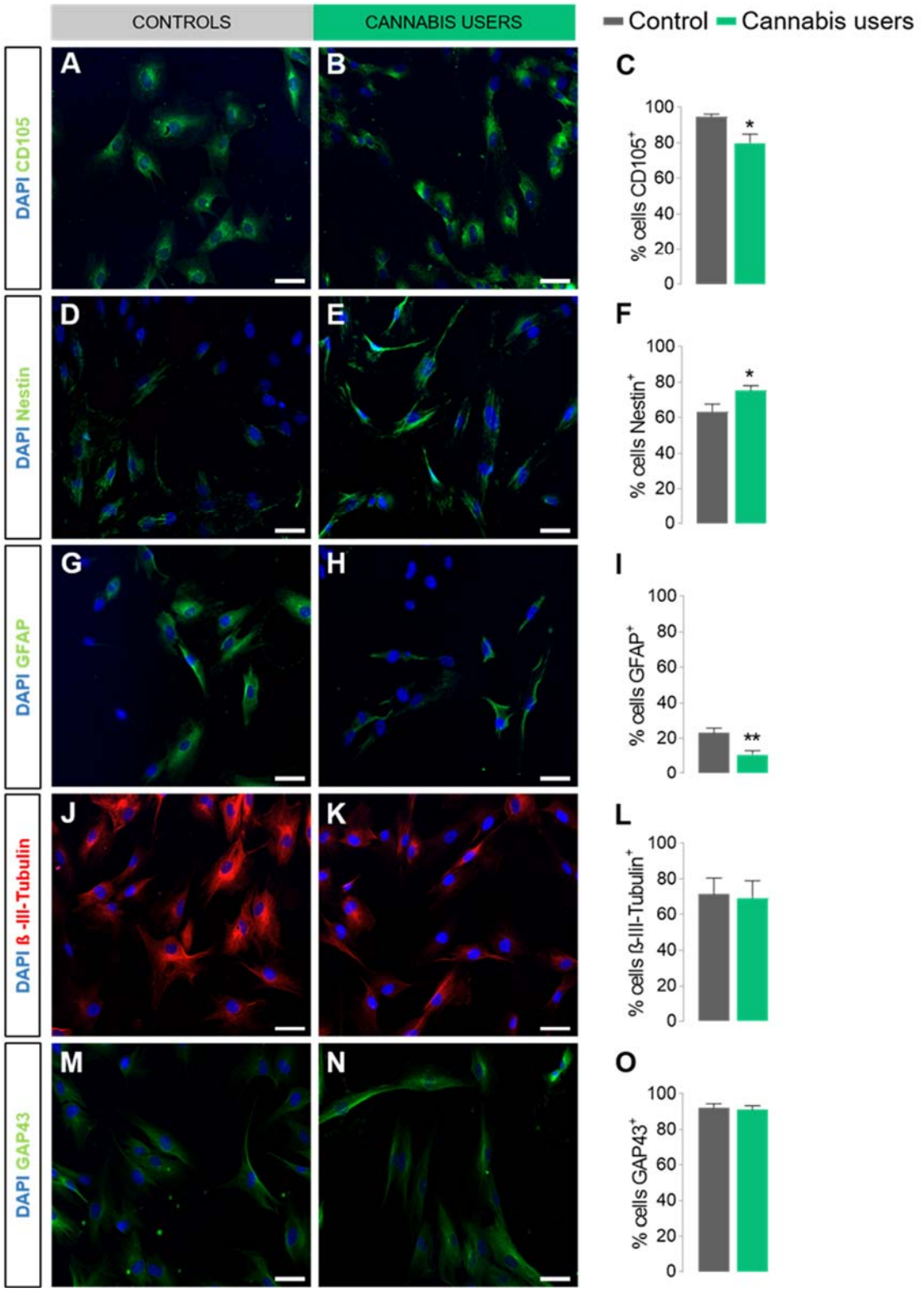


**Figure 2. Cell types derived from the olfactory neuroepithelium (ON) of cannabis users and control subjects**. Cells cultured to passage 6 were incubated for 24 hours under proliferative conditions. Representative immunofluorescence images and quantification of the different cell populations derived from a control subject and a cannabis user. Specific cell populations are immunolabelled in green or red and the nuclei are stained with DAPI. The quantification of the cells in each population is represented relative to the total cells ($DAPI^+$): **(A-C)** Mesenchymal $CD105^+$ cells; **(D-F)** $Nestin^+$ neural progenitor cells; **(G-I)** Glial-like $GFAP^+$ cells. **(J-L)** Immature β-III-Tubulin neurons; **(M-O)** Immature $GAP43^+$ neurons. Scale bar = 50µm. * $p < 0.05$; ** $p < 0.001$ (*Student's t-test*, n=5).

**FIGURE 3**

**A. Top Canonical Pathways**

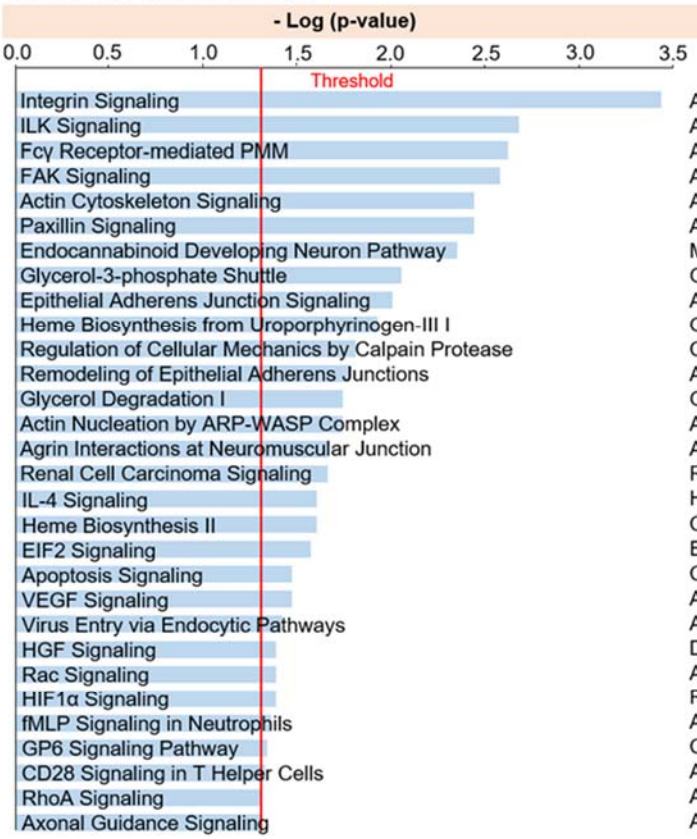


| | Proteins | Ratio |
|---|---|---|
| Integrin Signaling | ACTG1,ARPC2.DOCK1,ILKAP,RAP1B | 2.34 |
| ILK Signaling | ACTG1,DOCK1,FERMT2,ILKAP | 2.09 |
| Fcγ Receptor-mediated PMM | ACTG1,ARPC2,DOCK1 | 3.19 |
| FAK Signaling | ACTG1,DOCK1,RAP1B | 3.16 |
| Actin Cytoskeleton Signaling | ACTG1,ARPC2,DOCK1,RAP1B | 1.83 |
| Paxillin Signaling | ACTG1,DOCK1,RAP1B | 2.75 |
| Endocannabinoid Developing Neuron Pathway | MGLL,RAP1B,STMN2 | 2.61 |
| Glycerol-3-phosphate Shuttle | GPD2 | 33.3 |
| Epithelial Adherens Junction Signaling | ACTG1,ARPC2,RAP1B | 1.96 |
| Heme Biosynthesis from Uroporphyrinogen-III I | CPOX | 25 |
| Regulation of Cellular Mechanics by Calpain Protease | CDK1,RAP1B | 3.03 |
| Remodeling of Epithelial Adherens Junctions | ACTG1,ARPC2 | 2.9 |
| Glycerol Degradation I | GPD2 | 16.7 |
| Actin Nucleation by ARP-WASP Complex | ARPC2,RAP1B | 2.78 |
| Agrin Interactions at Neuromuscular Junction | ACTG1,RAP1B | 2.56 |
| Renal Cell Carcinoma Signaling | RAP1B,SLC2A1 | 2.5 |
| IL-4 Signaling | HLA-DQB1,RAP1B | 2.35 |
| Heme Biosynthesis II | CPOX | 11.1 |
| EIF2 Signaling | EIF4A1,RAP1B,RPL29 | 1.34 |
| Apoptosis Signaling | CDK1,RAP1B | 2.02 |
| VEGF Signaling | ACTG1,RAP1B | 2 |
| Virus Entry via Endocytic Pathways | ACTG1,RAP1B | 1.87 |
| HGF Signaling | DOCK1,RAP1B | 1.8 |
| Rac Signaling | ARPC2,RAP1B | 1.8 |
| HIF1α Signaling | RAP1B,SLC2A1 | 1.77 |
| fMLP Signaling in Neutrophils | ARPC2,RAP1B | 1.72 |
| GP6 Signaling Pathway | COL9A2,RAP1B | 1.68 |
| CD28 Signaling in T Helper Cells | ARPC2,HLA-DQB1 | 1.67 |
| RhoA Signaling | ACTG1,ARPC2 | 1.63 |
| Axonal Guidance Signaling | ARPC2,DOCK1,RAP1B,SRGAP1 | 0.82 |

**B. Top Diseases and Bio Functions**

| 1. Molecular and Cellular Functions | p-value range | Proteins |
|---|---|---|
| Cellular Development | 3.66E-02 - 1.69E-05 | 18 |
| Cellular Growht and Proliferation | 3.66E-02 - 1.69E-05 | 19 |
| Cellular Function and Maintenance | 3.93E-02 - 2.42E-05 | 25 |
| Cellular Assembly and Organization | 3.93E-02 - 2.87E-05 | 25 |
| Cell Morphology | 3.93E-02 - 5.23E-04 | 18 |

| 2. Physiological System Development and Function | p-value range | Proteins |
|---|---|---|
| Nervous System Development and Function | 3.66E-02 - 1.69E-05 | 19 |
| Tissue Development | 3.93E-02 - 1.69E-05 | 21 |
| Organ Morphology | 3.93E-02 - 1.81E-03 | 17 |
| Reproductive System Development and Function | 3.38E-02 - 1.81E-03 | 12 |
| Cell-mediated Immune Response | 3.66E-02 - 1.96E-03 | 3 |

| 3. Diseases and disorders | p-value range | Proteins |
|---|---|---|
| Cancer | 3.93E-02 - 5.41E-06 | 64 |
| Organismal Injury and Abnormalities | 3.93E-02 - 5.41E-06 | 64 |
| Gastrointestinal Disease | 3.93E-02 - 2.18E-05 | 60 |
| Developmental Disorder | 3.93E-02 - 6.82E-04 | 13 |
| Hereditary Disorder | 2.98E-02 - 6.82E-04 | 17 |

**Figure 3. Functional classification of the proteins differentially expressed in the olfactory neuroepithelium (ON) cells from cannabis users.** Differentially expressed proteins were analyzed with the Ingenuity Pathways Analysis (IPA) software. **(A)** Proteins differentially expressed are involved in 30 canonical pathways, sorted by the p-values assigned by IPA. These pathways have p-values above the red line threshold and thus, they are predicted to be affected. The ratio indicates the number of differentially expressed proteins found relative to the total number of proteins involved in the pathway. **(B)** The proteins differentially expressed that are involved in the diseases and functions are indicated. The p-value range and number of proteins involved in each disease or activity are included.

**FIGURE 4**

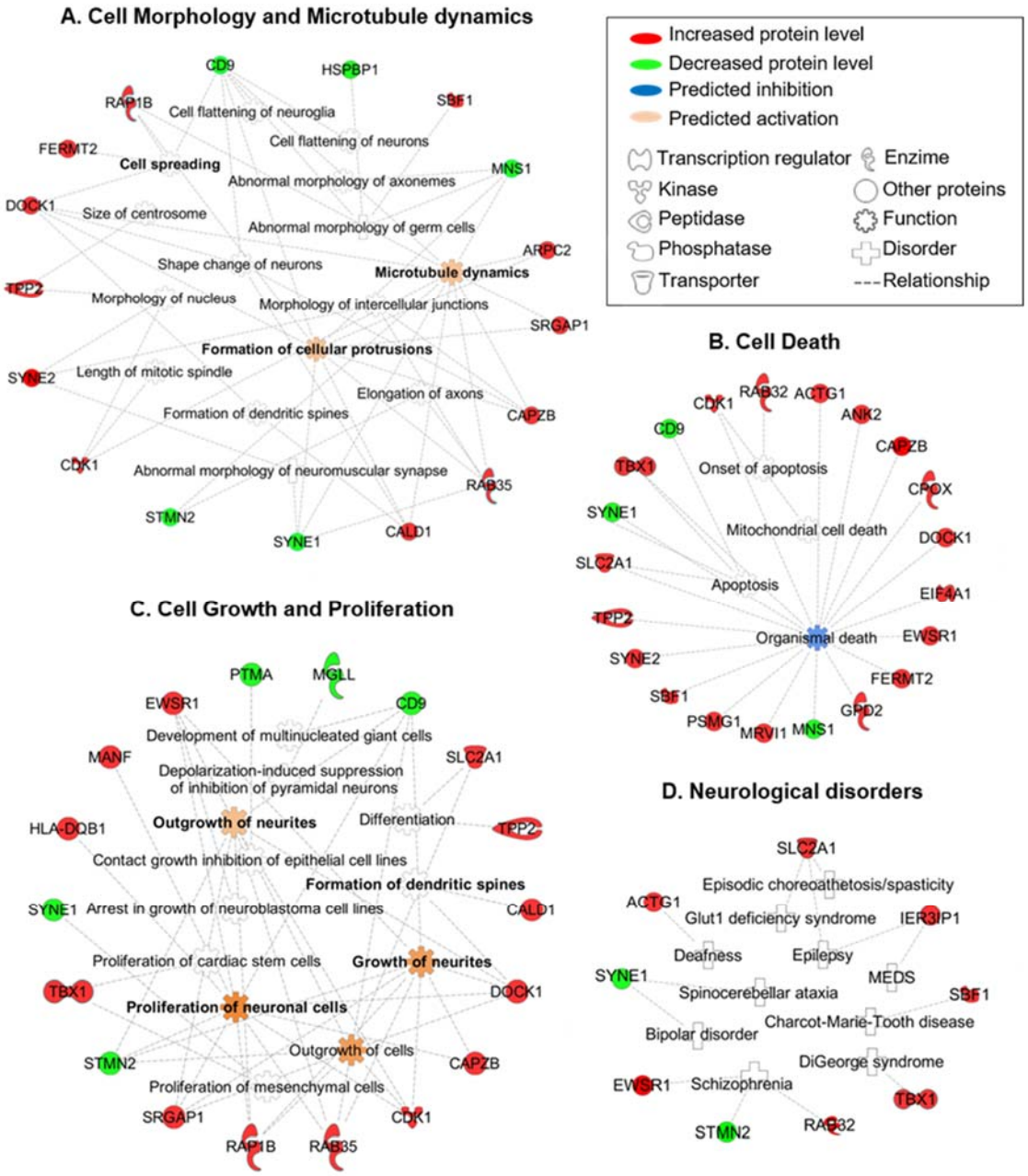


**Figure 4. Graphical correlations between differentially expressed proteins in olfactory neuroepithelium (ON) cells from cannabis users and their main related functions or diseases**. The pathways were obtained from the Ingenuity Pathways Analysis (IPA) software. The proteins differentially expressed in the ON cells from cannabis users ($p < 0.05$) are involved in: **(A)** cell morphology and microtubules dynamics, **(B)** cell death, **(C)** cell growth and proliferation, and **(D)** hereditary and/or developmental neurological disorders. Proteins with enhanced expression are indicated in red and the more weakly expressed proteins are indicated in green. Based on the literature and databases, the functions that are predicted to be activated or inhibited are labelled in orange or blue, respectively. The type of proteins, functions or diseases are indicated by different shape icons. MED: Microcephaly, epilepsy and diabetes syndrome.

**FIGURE 5**

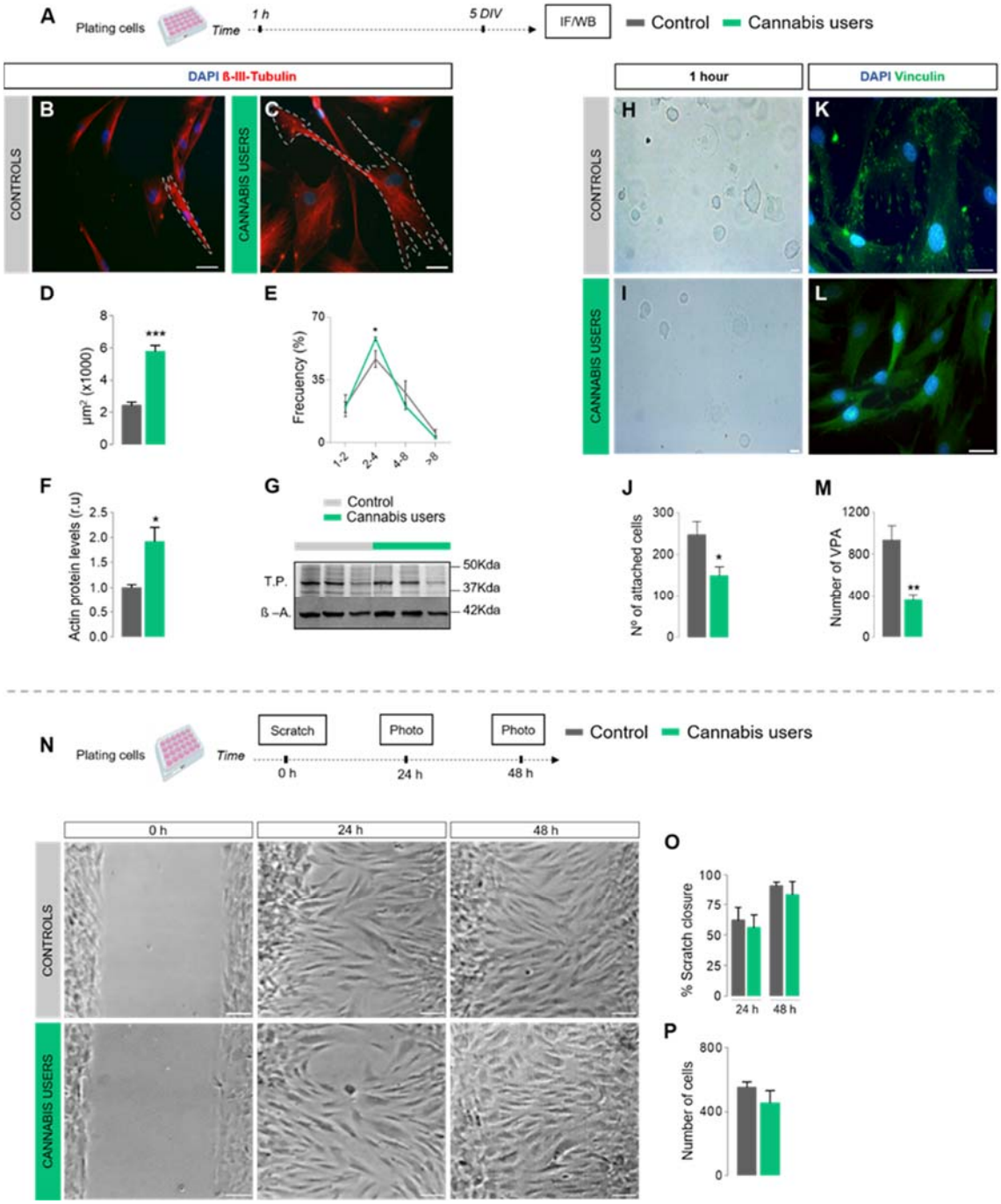


**Figure 5. Analysis of the olfactory neuroepithelium (ON) cell's cytoskeletal morphology, adhesion and migration. (A)** Cells were incubated for 1 hour or 5 days under proliferative conditions, after which they were analysed by immunofluorescences (IF) or in western blots (WB). **(B, C)** Representative immunofluorescence images of cultured cells derived from a control subject and a cannabis user, stained with anti- β-III-Tubulin (red) and DAPI (blue). The area and perimeter of cells were quantified by defining the stained area with ImageJ (dotted lines) **(D)** Quantification of cell area. **(E)** Quantification of the percentage of cells with specific roundness value intervals. **(F, G)** Quantification of β-actin (β-A) by western blots (r.u. = relative units) normalized to the total protein content (TP). **(H, I)** Representative bright field images of cells 1 hour after plating. **(J)** Quantification of the number of attached cells 1 hour after plating. **(K, L)** Representative immunofluorescence images of cells in culture derived from a control subject and a cannabis user, stained for vinculin (green) and with DAPI (blue). **(M)** The number of vinculin points of adhesion (VPA) were quantified. **(N)** Representative bright field images at 0, 24 and 48 hours after scratching the cell monolayer. **(O)** Quantification of the percentage of closure in the wound

area at 24 and 48 hours, relative to the baseline (t: 0h). **(P)** Quantification of the number of cells that migrated into the scratched area 24 h after scratching. Scale bar = 50 µm. * $p < 0.05$; ** $p < 0.001$; *** $p < 0.001$ (*Student's t-test*, n=5).

**FIGURE 6**

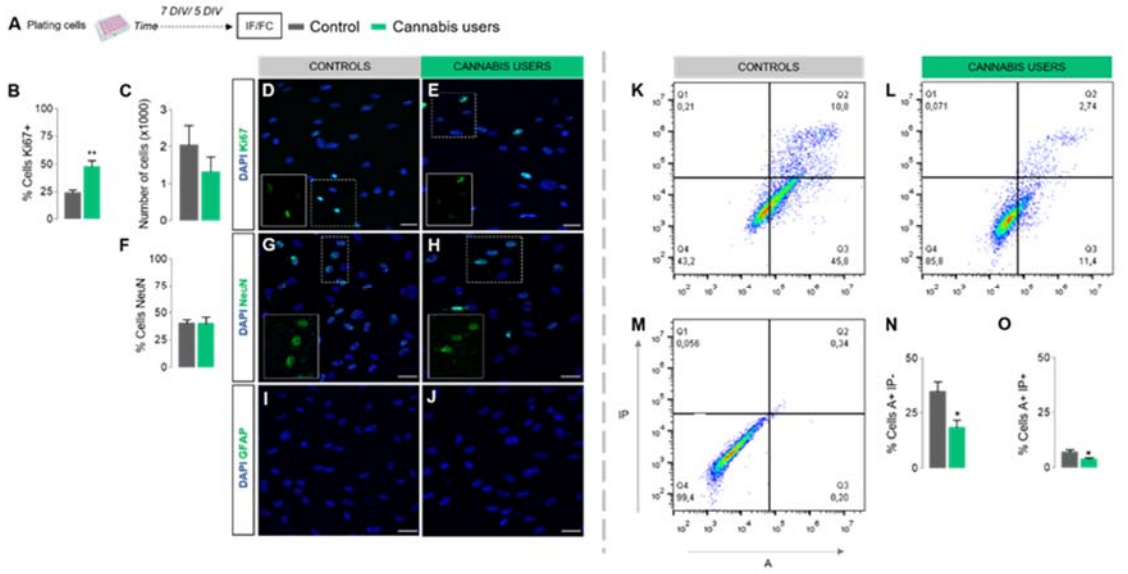


**Figure 6. Analysis of the olfactory neuroepithelium (ON) cell's proliferation, differentiation and apoptosis. (A)** Cells were incubated for 5 days under proliferative conditions, after which they were analysed by immunofluorescences (IF) or by flow cytometry (FC). **(B)** Quantification of proliferative Ki67$^{+}$ cells relative to the total number of cells (DAPI$^{+}$). **(C)** Quantification of the total number of cells (DAPI$^{+}$) in the culture**. (D, E)** Representative immunofluorescence images of cells in culture derived from control subjects and cannabis users. Cells under proliferation are immunolabelled in green (Ki67$^{+}$) and nuclei are stained in blue (DAPI). Selected areas marked with dotted lines are showed in the white squares with the green labelling alone. **(F)** Quantification of differentiated NeuN$^{+}$ cells relative to the total number of cells (DAPI$^{+}$). **(G-J)** Representative immunofluorescence images of cells in culture derived from control subjects and cannabis users. Differentiated NeuN$^{+}$ and GFAP$^{+}$ cells are immunolabelled in green and nuclei are stained with DAPI (blue). Selected areas marked with dotted lines are showed in the white squares with the green labelling alone. **(K-L)** Representative flow cytometry plots of cells in culture derived from control subjects and cannabis users. **(M)** ON cells were labelled with Annexin V (A) and Propidium Iodide (PI) followed by flow cytometric analysis to measure apoptosis. The percentage of the following cell populations is indicated: A-/PI- are viable cells (lower left quadrant); A+/PI- are early apoptotic cells (lower right quadrant); and A+/PI+ are late apoptotic cells (upper right quadrant). **(N)** Quantification of the percentage of cells in early (A+/PI-) and **(O)** late (A+/PI+) apoptosis. Scale bar = 50 µm. * $p < 0.05$; ** $p < 0.001$; (*Student's t-test*, n=5).